Distribution of End Groups within a Dendritic Structure: A SANS Study Including Contrast Variation

S. Rosenfeldt, N. Dingenouts, and M. Ballauff*

Polymer-Institut, Universität Karlsruhe, Kaiserstrasse 12, D-76128 Karlsruhe, Germany

N. Werner and F. Vögtle

Kekulé-Institut für Organische Chemie und Biochemie, Universität Bonn, Gerhard-Domagk-Strasse 1, D-53121 Bonn, Germany

P. Lindner

Institut Laue-Langevin, B.P. 156X, 38042 Grenoble Cedex, France

Received April 12, 2002; Revised Manuscript Received July 5, 2002

ABSTRACT: We present an analysis of the distribution of end groups within a urea-functionalized poly(propyleneamine) dendrimer of the fourth generation by small-angle neutron scattering (SANS). The phenyl end groups have been deuterated to enhance their contrast. The SANS experiments are performed using solution of the labeled dendrimer in mixtures of protonated and deuterated dimethylacetamide (DMA). In this way the contrast between the solute and the solvent is varied in a systematic fashion (contrast variation). The analysis presented here gives three partial scattering functions that depend differently on contrast. From these data, the scattering length density within the dendritic structure can be derived. All results show that the end groups are dispersed throughout the dendrimer with a broad maximum located at a radial distance that corresponds to ca. half of the overall size of the molecule. Hence, there is no well-defined surface of a dendritic structure defined by the end groups, but the end groups are mostly folded back into the interior of the molecule. These results, which are in full accord with the dense-core picture of dendrimers, are supported by recent theoretical deductions and simulations on the structure of dendrimers.

I. Introduction

Dendrimers are synthetic well-defined branched macromolecules that have aroused considerable interest in recent years. Their treelike architecture is formed by a stepwise interative reaction that starts out from a multifunctional core molecule.[1−5] A key problem in the field of dendrimers is their spatial structure and the location of the end groups. Most of the dendritic structure synthesized so far are composed from flexible units and the entire structure can assume an enormous number of conformations. A quantitative determination and understanding of the average conformation of dendrimers in solution is of central importance when discussing possible applications of these molecules.

The location of the terminal groups has been the subject of a long-standing controversy in the field. The first theoretical treatment by de Gennes and Hervet started from the assumption that all subsequent branches extend to the periphery of the molecule.[6] As the consequence of this assumption a limiting generation is predicted due to the steric hindrance of the end groups in the shell. This "dense-shell" picture has first been questioned by Lescanec and Muthukumar who showed that the distribution of segments has its maximum in the center of the molecule.[7] Hence, dendrimers exhibit a fluctuating structure and a part of the end groups are folded back into the interior of the molecule. This "dense-core" picture of dendrimers has been corroborated by a great number of theoretical studies.[8−18] In particular, the end groups are predicted to be dispersed throughout the structure. This distribution is not uniform, however, but there is a maximum at approximately half of the maximum radius of the molecule which originates from the backfolding of the end groups. Discussions of the distribution of end groups may be found in the work of Boris and Rubinstein[11] and in more recent work.[17,18] The theoretical understanding of dendritic structures seems to be well-developed by now and supports unambiguously the dense-core picture. A survey has recently been given in ref 19.

Small-angle neutron scattering (SANS; ref 20) as well as small-angle X-ray scattering (SAXS; ref 21) are the most powerful tools available to elucidate the spatial structure of dissolved dendrimers. Recent investigations by SANS have indeed corroborated the dense-core picture of dendrimers.[22−24] The segment density is shown to decay smoothly from the center of the molecule if the number of generations is low, i.e., for dendrimers of the fourth and fifth generations.[22,23] This finding is fully supported by a recent study of the interaction of dendrimers of fourth generation in solution by SANS.[25] Higher generations exhibit a more compact distribution of segments that may be modeled in first approximation by a dense sphere.[24]

The location of the end groups of the dendritic structures is less well investigated experimentally. SANS is the optimal tool to probe the location of end groups in a dendrimer because their contrast can be greatly enhanced by deuteration. Using SANS, Topp et al. studied poly(amido amine) dendrimers having deuterated end groups. These authors discussed the change of the radius of gyration when going from protonated to deuterated end groups.[26] They found that the radius of gyration of a dendrimer of seventh generation was increased significantly by deuteration of the end groups. From this finding, they concluded that the end groups

10.1021/ma020585c CCC: $22.00
Published on Web 09/12/2002

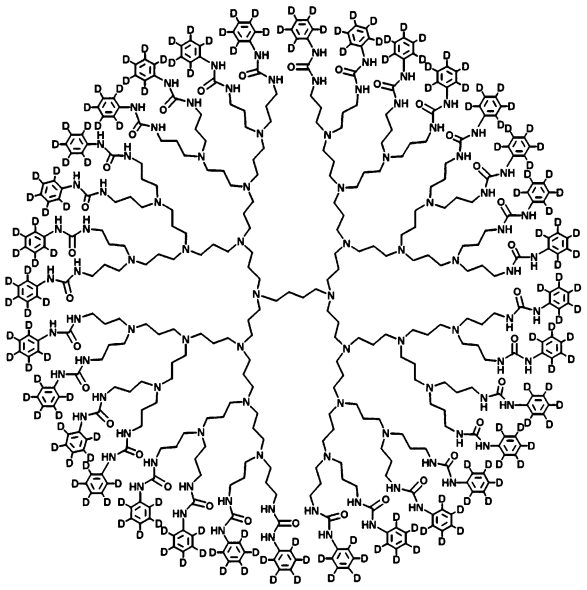

Figure 1. Chemical structure of the urea-functionalized poly(propyleneamine) dendrimer of the fourth generation G4-D having deuterated end groups.

are preferably located at the outside of the dendrimer.[26] This is in clear contradiction to the dense-core picture as already noted by the authors. Lyulin, Davies, and Adolf, however, showed that arguments solely based on the radius of gyration are not conclusive.[17] More recently Rietveld at al. presented a SANS study of dendrimers of generation 4 and 5 bearing deuterated end groups.[27] These authors measured the scattering intensities of the labeled dendrimers at different contrast and dicussed the radii of gyration thus obtained. The interpretation of these results was rendered difficult due to the presence of charges. Hence, the experimental studies presented so far do not allow a firm conclusion with regard to the location of the end groups in dendrimers.

Here we present a comprehensive SANS investigation devoted to a flexible dendrimer of the fourth generation having deuterated end groups. Figure 1 displays the chemical structure of the urea-functionalized poly(propyleneamine) dendrimer termed G4-D. The same dendrimer but with protonated end groups (G4-H) was recently studied extensively by use of SANS and shown to be without defects.[28,29] All phenyl end groups of G4-D studied have been fully deuterated to enhance their contrast toward the dendritic scaffold. It should be noted that no charged groups are present in G4-H or G4-D in order to avoid all complications due to the strong electrostatic interaction of charged dendrimers.[30,31] Moreover, the chemical structure of G4 is approximately centrosymmetrical, which facilitates the analysis of the SANS data. It is the goal of the present investigation to derive the full distribution of the end groups from SANS measurements. The contrast between the solute and the solvent is varied in a systematic fashion in the course of the analysis of G4-H and G4-D (contrast variation[19,21−23,32]). It will become apparent that the comparison of the deuterated and the protonated dendrimer G4 unambiguously leads to the localization of the end groups.

II. Theory

A. Contrast Variation. The analysis presented here rests fully on the technique of contrast variation. Hence, it is expedient to summarize the main points and the pertinent equations.[19,21] A comprehensive discussion of contrast variation and its application to dissolved polymeric structures was given recently in ref 19.

We consider a solution of monodisperse molecules in solution. The scattering intensity $I(q)$ ($q = (4\pi/\lambda)\sin(\theta/2)$; λ, wavelength of the incident neutrons; θ, scattering angle) can be written as[23,28]

$$I(q) = \frac{N}{V} I_0(q) S(q) + \frac{N}{V} I_{\mathrm{incoh}} \tag{1}$$

where N/V is the number density of dendrimers in the sample, $I_0(q)$ is the intensity of the dendrimers measured at infinite dilution. It is directly related to the spatial scattering length density distribution $\rho(\vec{r})$ of the dissolved objects. $S(q)$ is the structure factor containing the information about the correlations in wavenumber space. For the dendrimer G4 under consideration here $S(q)$ has recently been discussed in great detail.[28,29] In principle, $S(q)$ depends on contrast.[33] The data obtained for the present system, however, demonstrate that this influence is negligible (see below). Therefore, eq 1 can be used to describe the alterations by finite concentrations (see below). The term I_{incoh} denotes the q-independent incoherent contribution of a single particle.

To calculate the scattering intensity of the dissolved objects, the scattering length density distribution $\rho(\vec{r})$ is split up into a shape function $T(\vec{r})$ and the local scattering length density distribution $\rho_p(\vec{r})$ (cf. refs 19 and 21)

$$\rho(\vec{r}) = T(\vec{r})\rho_p(\vec{r}) + \rho_m[1 - T(\vec{r})] \tag{2}$$

where ρ_m is the scattering length density of the solvent. The shape function $T(\vec{r})$ described the cavity into which the solvent cannot penetrate whereas $\rho_p(\vec{r})$ is the scattering length density of the object in vacuo. The volume V_p is therefore given by the volume integral over $T(\vec{r})$ and the average scattering length density $\bar{\rho}$ is given by

$$\bar{\rho} = \frac{1}{V_p}\int T(\vec{r})\rho_p(\vec{r})\,\mathrm{d}\vec{r} \tag{3}$$

With these definitions, the excess scattering length density $\rho(\vec{r}) - \rho_m$ may be split into two terms:

$$\rho(\vec{r}) - \rho_m = T(\vec{r})[\bar{\rho} - \rho_m] + T(\vec{r})\Delta\rho(\vec{r}) \tag{4}$$

From this definition it follows that the volume integral over $T(\vec{r})\Delta\rho(\vec{r})$ must vanish.

Evidently, eq 4 holds true for a given conformer of the dendrimer that is oriented with regard to a fixed direction in space. The calculation of the measured intensity involves therefore the averaging over all conformers present in the solution and the average over all orientations with regard to the direction of $\vec{q}$.[21] Together with eq 4 this leads to the scattering intensity $I_0(q)$ of a single particle, which may be split into three terms:

$$I_0(q) = (\bar{\rho} - \rho_m)^2 I_S(q) + (\bar{\rho} - \rho_m) I_{SI}(q) + I_I(q) \tag{5}$$

The first term that scales with the square of the contrast $\bar{\rho} - \rho_m$ depends only on the shape function.[19] Hence, contrast variation leads to a splitting of the measured intensity into a term that only depends on shape and two additional contributions that are related to the

distribution of the scattering length density $\rho_p(\vec{r})$ within the structure.

It is clear that $\bar{\rho}$ does not depend on the conformation of the molecule but remains invariant under all conditions. Therefore, the decomposition of the intensity according to eq 5 can be done for systems consisting of many conformers. If there is a polydispersity of sizes and/or of chemical structures, however, $\bar{\rho}$ is not a constant anymore and the above separation does not work properly anymore.

From Figure 1, it is evident that the dendrimers G4-H and G4-D are approximately centrosymmetrical. Hence, there average density distribution can be described by a radial symmetric function. This amounts to the description of the dendritic structure in terms of a mean-field approach that neglects all fluctuations around the average distribution (see the discussion in ref 11). If the structure exhibits marked fluctuations the mean-field approach is no longer valid and $\langle T(\vec{q})^2\rangle$ differs strongly from $\langle T(\vec{q})\rangle^2$. It must be kept in mind, however, that the dendrimers G4-H and G4-D are rather small compounds and no large deviations from the equilibrium structure are to be expected. This is also found directly in a simulation of the dendritic structure under consideration here showing that fluctuations are small in the case of G4.[34]

Hence, in the following $T(\vec{r})$ will be replaced by its statistical-mechanical average $T(r)$ which is only dependent on the distance r from the center of the molecule. Therefore

$$I_S(q) = T^2(q) \tag{6}$$

where

$$T(q) = \frac{4\pi}{q}\int_0^\infty r\,T(r)\,\sin(qr)\,\mathrm{d}r \tag{7}$$

It need to be noted that possible fluctuations will contribute to all three partial scattering functions enumerated in eq 5. Equation 2 holds also true for conformers deviating strongly from the average distribution, of course. Therefore, the scattering intensity due to these conformers will be contained in all terms of eq 5.

B. Treatment of Data. The above set of equation furnishes the basis for the evaluation of experimental data. First of all, eq 5 allows one to extrapolate the measured SANS data to infinite contrast where $I_0(q)$ is only determined by $T(r)$. It is clear that the deuteration of the end groups must not change $T(r)$ because the shape of the molecule should remain the same in order to apply the present analysis. A comparison of $T(r)$ of G4-H and G4-D may therefore serve for a sensitive test of the general validity of the procedure leading to $T(r)$.

Evidently, measurements at least three different scattering length densities ρ_m of the solvent are needed to determine the three partial scattering intensities enumerated in eq 5. If the incoherent contribution I_{incoh} can be obtained independently through data taken at high q values, the term $I_I(q)$ furnishes information about the deviation $T(\vec{r})\Delta\rho(\vec{r})$ of the average scattering length density $\bar{\rho}$. This variation will be most pronounced if the deuterated end groups are affixed to a protonated dendritic scaffold, otherwise $I_I(q)$ is expected to be small. $I_I(q)$ can be determined if the contrast $\bar{\rho} - \rho_m$ is low. A series of measurements of dendrimers taken at more than three different contrasts will serve for the secure evaluation of the three partial scattering functions $I_S(q)$, $I_{SI}(q)$, and $I_I(q)$ that contain all structural information. No particular contrast for which, e.g., the end groups are matched is needed.

The foregoing considerations hence suggest the following procedure:

1. The influence of finite concentration embodied in $S(q)$ is determined through SANS measurements at dendrimer concentrations up to concentrations of 40 g/L. The subsequent analysis will show that G4-D is characterized by the same shape function $T(r)$ as the protonated molecule G4-H investigated previously.[28,29] $S(q)$ is solely governed by $T(r)$ in this regime of concentrations,[25,29] the data of $S(q)$ determined experimentally for the deuterated dendrimer should coincide with data measured previously for the protonated compound G4-H.[28]

2. The previous analysis of G4-H has given a precise value for I_{incoh} of the fully protonated structure. This term is proportional to the number of H atoms in the chemical structure.[20] Hence, I_{incoh} of G4-D can be estimated by reducing I_{incoh} of G4-H according to the decreased number of hydrogen atoms. All data used in the subsequent steps are corrected for I_{incoh} (see below).

3. Data at low q may be extrapolated to vanishing scattering angle using Guinier's law[20]

$$I_0(q) = V_p^2(\bar{\rho} - \rho_m)^2\exp\left(-\frac{q^2R_g^2}{3}\right) \tag{8}$$

$I_0(0)$ may therefore serve to determine the volume V_p of the particle and hence its molecular weight M ($=V_p/\bar{v}$, $\bar{v}$: partial specific volume). Moreover, this analysis leads to the average scattering length density $\bar{\rho}$ necessary for the subsequent steps.

The radius of gyration itself is dependent on contrast through (see refs 19 and 21 and further references given there)

$$R_g^2 = R_{g,\infty}^2 + \frac{\alpha}{\bar{\rho} - \rho_m} + \frac{\beta}{(\bar{\rho} - \rho_m)^2} \tag{9}$$

Here the term $R_{g,\infty}$ is the radius of gyration of the distribution $T(\vec{r})$. The coefficient α is a measure of the distribution $T(\vec{r})\Delta\rho(\vec{r})$. It is given by

$$\alpha = \frac{1}{V_p}\int_0^\infty T(\vec{r})\Delta\rho(\vec{r})r^2d\vec{r} \tag{10}$$

where $\vec{r}$ is now the vector the origin of which is the center of gravity of the distribution $T(\vec{r})$. The coefficient β is zero for centrosymmetrical distributions and should hence vanish for the present dendrimers. Equation 9 demonstrates that the radius of gyration can only be discussed if the contrast $\bar{\rho} - \rho_m$ is known with sufficient accuracy. Going from a protonated to a deuterated dendritic structure, however, will profoundly change $\bar{\rho}$ and render a direct comparison of the measured radii of gyration R_g a difficult task.

4. In the next step, the measured scattering intensities are decomposed according to eq 5 to yield the three partial scattering functions. From $I_S(q)$ thus obtained, the shape function can be derived through use of eqs 6 and 7. $T(r)$ together with fits of the terms $I_{SI}(q)$ and $I_I(q)$ then lead to the distribution $\rho_p(r)$ as defined through eq 2, which describes the radial variation of the scattering length density. This function is directly coupled

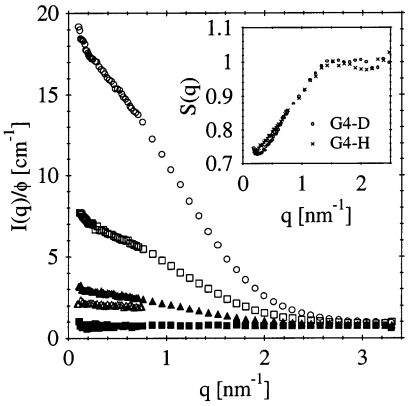

Figure 2. Measured scattering intensities $I(q)$ of protonated dendrimer G4-H. Parameter of the different curves is the contrast adjusted by mixtures of deuterated and protonated dimethylacetamide. The composition of DMA-D9 to DMA-H9 was (volume %) as follows: hollow circles, 100:0; hollow squares, 70:30; filled triangles, 50:50; filled squares, 25:75; hollow triangles, 0:100. The respective contrasts are gathered in Table 1. The concentration of the dissolved dendrimer was 40 g/L for all measurements. The inset shows the structure factor $S(q)$ derived experimentally for this concentration for G4-H (crosses) and for G4-D (hollow squares).

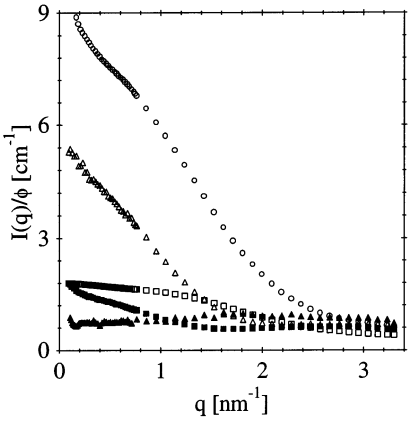

Figure 3. Measured scattering intensities of the partially deuterated dendrimer G4-D. Parameter of the different curves is the contrast adjusted by mixtures of deuterated and protonated dimethylacetamide. The composition of DMA-D9 to DMA-H9 was (volume %) as follows: hollow circles, 100:0; hollow squares, 70:30; filled triangles, 50:50; filled squares, 25:75; hollow triangles, 0:100. The respective contrasts are gathered in Table 1. The concentration of the dissolved dendrimer was 40 g/L for all measurements.

to the distribution of deuterated end groups because of their much enhanced contrast. It hence gives the desired information about the distribution of the end groups.

III. Experimental Section

The dendrimer G4 analyzed here was synthesized using the techniques described in ref 35. The deuterated dendrimer G4-D was synthesized using fully deuterated phenylisocyanate. Details of the synthesis and the characterization of the partially deuterated dendrimer G4 will be given elsewhere.

Protonated DMA (DMA-h_9, Fluka, analytical grade) and deuterated DMA (DMA-d_9, degree of deuteration: 99%, Deutero GmbH) were used as received. The specific volume of the dendrimer in DMA-h_9 was measured using a DMA-60-densitometer supplied by Paar (Graz, Austria). The specific volume of G4-D has the value $\bar{v} = 0.82$ cm^3/g in DMA-d_9.

All SANS data reported herein were measured using the D11 at the Institut-Laue-Langevin. All data have been circularly averaged and corrected using the software supplied by the ILL.

IV. Results and Discussion

A. Acquisition of Data. The present analysis rests on the determination of the scattering intensity of the dissolved dendrimers G4-H and G4-D at different contrasts with the highest precision possible. For low contrasts, however, the measured intensity is concomitantly smaller and the subtraction of the background (solvent and sample holder) more difficult to perform. Moreover, $I(q)$ must be securely determined up to high scattering angles, i.e., at q values beyond the Guinier region to arrive at meaningful conclusions. This requires a precise determination of the scattering by the solvent and a careful normalization of the data. Figures 2 and 3 show the corrected intensities of G4-H and G4-D, respectively. In both cases a strong dependence of the measured $I(q)$ is immediately visible. Moreover, the scattering intensities of the protonated and the deuterated dendrimer differ markedly. This marked effect provides a sound base for the subsequent analysis for the end group distribution.

In both cases $I(q)$ is converging to a low but finite value in the region of high q values. As already discussed in the course of our previous investigations[22,23,28,29] $I(q)$ measured at high scattering angles is dominated by the incoherent contribution I_{incoh} (see eq 1). Recently, I_{incoh} of G4-H has been determined with great precision from data taken at high q.[28] As described in the section Theory, a good estimate of I_{incoh} of G4-D can be obtained from this figure because the incoherent contribution is proportional to the number of hydrogen atoms in the dendritic scaffold. The estimate for G4-D thus obtained ($I_{incoh} = 0.55$ cm^{-1}) compare favorably with the average value of $I(q)$ measured at high q values of the deuterated dendrimer (cf. Figure 3; $I_{incoh} = 0.59$ cm^{-1}).

There are small differences of this background in the individual measurements, however. These differences are assigned to difficulties in the course of the subtraction of the background. An error in the length of the optical path (1 mm) of a few percent already would suffice to explain these residual differences seen for different contrasts at high q values. Hence, I_{incoh} is adjusted for each contrast to match $I(q)$ at the highest q value under consideration here (3.3 nm^{-1}). This background is subtracted from the data taken for a given contrast (cf. step 2 of the treatment of data). It should be kept in mind, however, that possible errors in the course of this subtraction may cause problems in the region of highest scattering angles where the coherent intensity is much smaller than I_{incoh}. This point will therefore be reconsidered further below.

After correcting the scattering intensities of G4-H and G4-D for I_{incoh}, the effect of finite concentration is removed by division through $S(q)$. The structure factor $S(q)$ has been determined previously with great precision.[28,29] The inset of Figure 2 displays the data of $S(q)$ obtained for G4-H in ref 28 (crosses). To check a possible influence[33] of contrast and internal deuteration onto $S(q)$, measurements of G4-D in fully deuterated DMA-D9 were performed here to obtain $S(q)$ directly. In the case of G4-H, $S(q)$ is related to the entire molecule while measurements of G4-D "see" mostly the deuterated end groups. Hence, there is a marked difference of contrast and a possible influence on $S(q)$ should be visible in this comparison. The resulting data are displayed in the

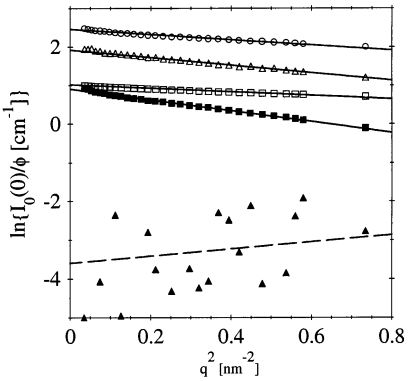

Figure 4. Guinier plots of dendrimer G4-D. Parameter of the different curves is the contrast adjusted by mixtures of deuterated and protonated dimethylacetamide. The composition of DMA-D9 to DMA-H9 was (volume %) as follows: hollow circles, 100:0; hollow squares, 70:30; filled triangles, 50:50; filled squares, 25:75; hollow triangles, 0:100. The respective contrasts are gathered in Table 1. All data have been corrected for I_{incoh}. Moreover, the effect of finite concentration has been corrected by division through the structure factor $S(q)$ (see Figure 2).

inset of Figure 2. There are small differences between the two sets of data. These differences, however, are within the experimental uncertainty. Evidently $S(q)$ is independent of the contrast within the particle as expected.[28] Hence, eq 1 can be used to account for the influence of concentration for the present system. The data obtained for G4-D (circles in inset of Figure 2) are therefore used for the correction for finite concentration as indicated above (cf. the discussion of step 1 in the section Treatment of Data).

There is an upturn of the measured intensities in the region of very small scattering angles ($q < 0.2$ nm^{-1}). This points to residual aggregates that cannot be avoided in SANS measurements of these systems. The problem has been discussed in great detail recently and criteria have been developed down to which scattering angle resonable data can be obtained.[28] In the present discussion, these data are omitted.

B. Guinier Regime. The data corrected for I_{incoh} and $S(q)$ are the absolute intensities $I_0(q)$ that refer to a single particle (see eq 5). Division through the volume fraction ϕ ensures proper normalization to the concentration. The volume fraction follows from the weight concentrations c through $\phi = c\bar{v}$ where $\bar{v}$ is the partial specific volume.

Figure 4 shows the Guinier plots (see eq 8) of the data of G4-D taken at different contrasts. The changes of the slope referring to the dependence of R_g on contrast are directly evident from this plot. In the case of dendrimer G4-H (not shown) no marked change of these slopes is seen experimentally (see also refs 22, 23). This immediately points to a variation of the scattering length density inside of the dendritic structure of G4-D which is analyzed further below.

The data referring to the lowest contrast (filled triangles in Figure 4) are insecure because in this case the incoherent scattering I_{incoh} exceeds the coherent part. Despite the large margin of error obvious from Figure 4, it is evident that the coherent scattering intensity increases with increasing q. This is expected in the immediate neighborhood of the match point (see eq 9). As a consequence, R_g^2 must assume a negative value which is also evident from Figure 4. The data obtained near the match point, however, are not sufficient to determine the radius of gyration with sufficient accuracy. Hence, only an estimate of the forward scattering $I_0(0)$ is taken from the Guinier plot of this set of data. Table 1 gathers the measured radii of gyration.

Table 1. Radii of Gyration of G4 Measured at Different Contrast

	G4-H		G4-D	
vol %[a]	$\Delta\rho$ (10^{10} cm^{-2})[b]	R_g (nm)[c]	$\Delta\rho$ (10^{10} cm^{-2})[d]	R_g (nm)[e]
100	−5.02	1.6 ± 0.1	−3.39	1.4 ± 0.1
70	−3.05	1.6 ± 0.1	−1.47	1.2 ± 0.2
50	−1.87	1.6 ± 0.2	−0.16	
25	−0.38	2.0 ± 0.2	1.25	1.8 ± 0.3
0	1.01	1.4 ± 0.2	2.65	1.7 ± 0.1

[a] Volume of DMA-D9 in mixture with DMA-H9. [b] $\Delta\rho$:contrast given by $\bar{\rho} - \rho_m$. [c] Radius of gyration. [d] $\Delta\rho$: contrast given by $\bar{\rho} - \rho_m$. [e] Radius of gyration.

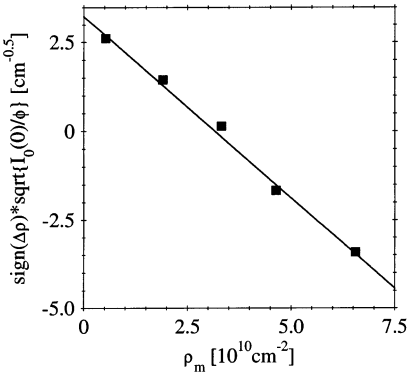

Figure 5. Determination of V_p and $\bar{\rho}$ by contrast variation. The squareroot of the intensity extrapolated to vanishing scattering angle (see Figure 4) is plotted against the scattering length density ρ_m of the solvent. All data have been multiplied by the sign of the respective contrast (see Table 1). The different contrast of the solvent was adjusted through mixtures of protonated and deuterated dimethylacetamide. The slope of the straight line gives V_p whereas the intercept leads to $\bar{\rho}$ (see eq 8).

Since the correction for I_{incoh} has already been done, the intercepts yield directly $I_0(0)$ as the function of contrast.[28] Figure 5 displays $I_0(0)^{1/2}$ as the function of the scattering length density ρ_m of the solvent. This plot shows that eq 8 is valid for $q = 0$ as expected. The slope yields $V_p = 9.7 \pm 0.6$ nm^3 as the volume of a single dendrimer. Together with the partial molar volume $\bar{v}$ this gives a molecular weight of 7.110 ± 330. This is identical to the theoretical molecular weight (7.487) within the given limits of error. The same holds true for the average contrast $\bar{\rho}$ which follows from the intercept in Figure 5. Here we obtain $\bar{\rho} = (3.18 \pm 0.18) \times 10^{-10}$ cm^{-2} whereas the theoretical value is $\bar{\rho} = 3.17 \times 10^{-10}$ cm^{-2}. Both data indicate clearly that G4-D is a perfect monodisperse structure, no corrections for a possible polydispersity or structural faults need to be taken into consideration. The average scattering length density $\bar{\rho}$ determined experimentally in this way is now used for all subsequent steps in the analysis.

Figure 6 shows the Stuhrmann plot of the radii of gyration determined as the function of contrast (see Figure 4). As already mentioned above, R_g^2 taken in the immediate vicinity of the matchpoint has been omitted. The filled squares refer to G4-D whereas the hollow squares give the respective data of G4-H. Two features command attention in Figure 6: (i) Straight lines are obtained having the same slopes, and (ii) the intercepts are clearly different. The first point shows immediately

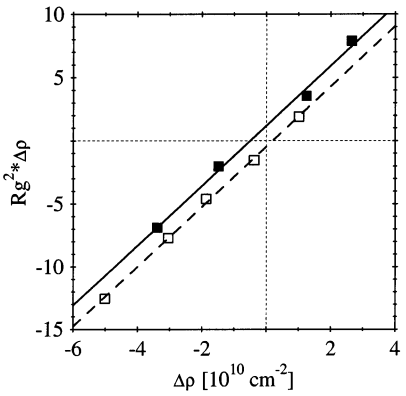

Figure 6. Stuhrmann plot of the radii of gyration R_g as a function of the contrast $\Delta\rho = \bar{\rho} - \rho_m$ of the solute dendrimer. The filled squares refer to the dendrimer G4-D whereas the hollow squares give the respective radii of gyration of G4-H. The different contrast of the solvent was adjusted through mixtures of protonated and deuterated dimethylacetamide. (see eq 8). The slope of lines yield $R_{g,\infty}^2$ whereas the intercept leads to α according to eq 9. The values of R_g have been determined by the Guinier plots shown in Figure 8.

Table 2. Parameters Characterizing Dendrimers G4-D and G4-H

		M_w (g/mol)			$\bar{\rho}$ (10^{10} cm^{-2})	
	V_p [nm^3]	exptl	theor	$R_{g,\infty}$ [nm]	exptl	theor
G4-H	9.9 ± 0.3	7100 ± 220	7326	1.5 ± 0.2	1.5 ± 0.1	1.52
G4-D	9.7 ± 0.6	7110 ± 330	7487	1.5 ± 0.2	3.2 ± 0.2	3.18

that the coefficient β is zero as expected for a centrosymmetrical chemical structure. It constitutes the experimental proof that noncentrosymmetrical conformations of the dendrimer can play no major role. This underscores the analysis of the scattering data in terms of centrosymmetrical functions as, e.g., $T(r)$ and $\rho_p(r)$ despite the fact that noncentrosymmetrical conformations are not ruled out totally.

Figure 6 demonstrates that the slope of the lines, i.e., $R_{g,\infty}$ does not change upon deuteration. This clearly indicates that the overall dimensions of the dendrimer as expressed through $R_{g,\infty}$ remain unaltered upon substituting the hydrogen atom of the end groups by deuterons. The H/D substitution is a rather small change of the molecule in the present case but Figure 6 gives a clear proof that this is the case indeed. The intercept α, which is virtually zero for the protonated dendrimer G4-H, is positive for G4-D. This can immediately be traced back to the fact that the internal scattering length density $\rho_p(r)$ (see eq 2) must increase with increasing radial distance r from the center of the molecule. It points to the fact that the deuterated end groups that contribute most to $\rho_p(r)$ are located preferably at larger distances from the center. No further conclusion, however, can be drawn from this finding that is solely based on data taken in the Guinier region. Table 2 displays the main parameters obtained from the analysis of the Guinier region.

C. Partial Scattering Functions. Having determined the average scattering length density $\bar{\rho}$ of G4-D we now turn to the evaluation of the partial scattering functions $I_S(q)$, $I_{SI}(q)$, and $I_I(q)$ defined through eq 5. The entire information to be obtained by a scattering experiment is embodied in these functions. These terms can be obtained by fits of all scattering curves obtained at five different contrasts (see Figure 3) for a given value of q. The system of equations is overdetermined and the fit of eq 5 presents a consistency check at the same time. It must be kept in mind, however, that the numerical procedure based on eq 5 to extract these functions from experimental data is rather difficult. At high contrast the shape term $I_S(q)$ will be dominant whereas at low contrast the problem of background subtraction may lead to appreciable errors in the determination of $I_{SI}(q)$ and $I_I(q)$. Moreover, eq 5 can only be applied for practically monodisperse systems. There is an additional criterion, however, that helps to extract meaningful results from scattering data: General theory demonstrates that the cross term $I_{SI}(q)$ as well as the term $I_I(q)$ of eq 5 must vanish in the limit $q = 0$.[19] This condition helps to assess the data derived for small q values which may be afflicted by errors due to the correction for finite concentration.

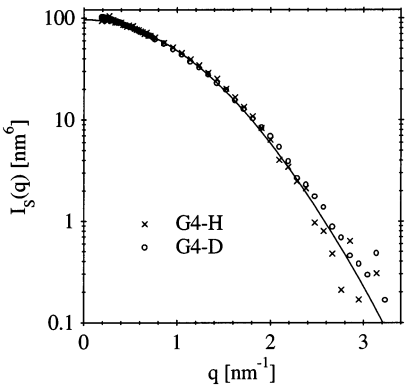

Figure 7. Partial intensity $I_S(q)$ (cf. eq 5) determined by contrast variation for dendrimer G4-H (crosses; see also ref 28) and for G4-D (hollow circles) obtained here. The solid line shows the fit of the data by a Gaussian defined in eq 11.

Figure 7 shows the shape term $I_S(q)$ derived for the protonated dendrimer G4-H (crosses)[28] and for the deuterated compound G4-D obtained herein. Both sets of experimental data agree as expected. The term $I_S(q)$ is not altered throughout the entire q range. The conclusion to be drawn from this finding hence exceeds the statement made above from an analysis of the Guinier region which is related only to the overall shape of the molecule.

As already found for G4-H in previous analyses $I_S(q)$ can be described by a Gaussian throughout the entire q range:[25,29]

$$I_S(q) = V_p^2 \exp\left(-\frac{q^2 R_{g,\infty}^2}{3}\right) \qquad (11)$$

The solid line shows the fit of this expression to the data of G4-D. It shows that the experimental data obtained for $I_S(q)$ can be fully described by eq 11. Therefore, $T(r)$ is a Gaussian as well and can be rendered as[25,29]

$$T(r) = V_p\left(\frac{3}{2\pi R_{g,\infty}^2}\right)^{3/2} \exp\left(-\frac{3r^2}{2R_{g,\infty}^2}\right) \qquad (12)$$

This demonstrates that the maximum density is located in the center of the molecule and not in the periphery.[23]

The other partial scattering functions $I_{SI}(q)$ and $I_I(q)$ defined through eq 5 obtained for G4-D are shown in Figure 8. Each term tends to zero for small and for large scattering angles as expected. The cross term is negative. $I_I(q)$ is found to be positive as it should be. The accuracy of $I_{SI}(q)$ is better than the one of $I_I(q)$ because

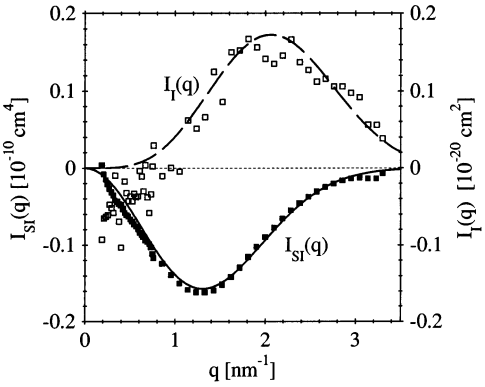

Figure 8. Partial scattering functions $I_{SI}(q)$ (filled squares) and $I_I(q)$ (hollow squares) as a function of q (see eq 5).

the contribution of the cross term to the measured intensity scales linear with the contrast. In the case of $I_I(q)$ the data are insecure for small q because of the reasons indicated above. Nevertheless, the decomposition according to eq 5 is possible for the present set of data and leads to reasonable results.

D. Fit of $\rho_p(r)$ and Localization of End Groups. The analysis of the measured intensities described in the previous sections clearly demonstrates that the partial deuteration of the end groups is followed by a marked change of the partial scattering functions $I_{SI}(q)$ and $I_I(q)$ while $I_S(q)$ remains unchanged. In principle, the information embodied in the term $I_I(q)$ together with $T(r)$ should fully suffice to derive the function $\rho_p(r)$ in an unambiguous manner. The limited accuracy of $I_I(q)$, however, renders the inversion of this term an impractical procedure. Therefore, the following method was used: A discrete trial distribution of $\rho_p(r)$ inspired by the theoretical prediction of ref 11 was set up. The shape function $T(r)$ has been determined very accurately from $I_S(q)$ before. Insertion of $T(r)\rho_p(r)$ into eq 4 and eq 5 leads to the calculated $I_{SI}(q)$ and $I_I(q)$. These results can directly be compared to the experimental data displayed in Figure 8. The trial distribution $\rho_p(r)$ is then changed until full agreement of the measured and the calculated terms $I_{SI}(q)$ and $I_I(q)$ is reached.

The determination of $\rho_p(r)$ is reliable for the following reasons: (i) The integral over $T(r)\rho_p(r)$ must give the experimental $\bar{\rho}$ according to eq 3. Given the shape function $T(r)$ that has already been determined accurately, eq 3 provides a stabilization for the procedure by which $\rho_p(r)$ is determined. (ii) Additional calculations have been done assuming totally different starting points that correspond e.g. to the dense shell picture of dendrimers. Here $\rho_p(r)$ would increase markedly at the outside of the molecule and assume its maximum value at the largest radial distances compatible with $T(r)$. Results obtained from these calculations are not in agreement with the present experimental data.

Figure 9 displays the distribution $\rho_p(r)$ obtained for dendrimer G4-D by this procedure. The distribution $\rho_p(r)$ may be viewed upon as the conditional probability for the scattering length density $\rho(r)$ of a given segment, i.e., the probability that a given segment has the scattering length density $\rho_p(r)$. The unconditional probability of finding a segment is the product $T(r)\rho_p(r)$. Since the deuterated end groups of G4-D have a much enhanced contrast as compared to the dendritic scaffold, $\rho_p(r)$ is directly proportional to the distribution of end groups in the dendrimer.

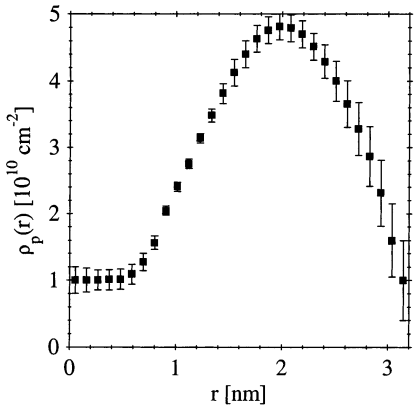

Figure 9. Distribution $\rho_p(r)$ determined from contrast variation.

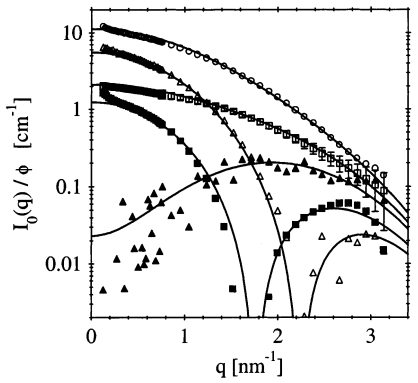

Figure 10. Comparison of the structural model to measured intensities: Corrected scattering intensities $I_0(q)/\phi$ as a function of q. Parameter of the different curves is the contrast adjusted by mixtures of deuterated and protonated dimethylacetamide. The composition of DMA-D9 to DMA-H9 was (volume %) as follows: hollow circles, 100:0; hollow squares, 70:30; filled triangles, 50:50; filled squares, 25:75; hollow triangles, 0:100. The respective contrasts are gathered in Table 1.

The function $\rho_p(r)$ exhibits a maximum at ca. 2 nm and decays monotonically for larger r. The greatest radial distance for which $T(r)$ is significantly greater than zero are approximately 3 nm. The maximum of ρ_p at ca. 2 nm demonstrates that the dense shell picture can be ruled out immediately. The resulting $\rho_p(r)$ obtained here, however, compares favorably with the distribution of end groups calculated in the frame of the theory of Boris and Rubinstein.[11] This shows that the present data are compatible with the dense core picture of dendrimers. Most of the end groups fold back, they are not located preferably at the surface of the molecule.

An important check of ρ_p can be achieved through comparing not only $I_{SI}(q)$ and $I_I(q)$ with calculated data but also the scattering functions $I_0(q)/\phi$ measured at different contrast. Figure 10 shows a comparison of the experimental intensities corrected for I_{incoh} with the intensities calculated for the respective contrast by use of $\rho_p(r)$ (cf. Figure 9). It is evident that the corrected experimental intensities have large error bars below 0.1 cm^{-1} because of the background subtraction. The comparison of theory and experiment is only significant above this value. Figure 10 shows, however, that theory gives the correct trends for all contrasts under consideration: The decrease of the intensity of scattering curves measured at low contrast is more marked in the vicinity of the match point because of a pronounced minimum. The position of the minima cannot be de-

tected securely because of the marked incoherent background. The scattering data in the reliable range ($I_0(q)/\phi > 0.1$ cm^{-1}), however, are fully compatible with the positions predicted by theory. Moreover, the position of the minimum is shifted to smaller scattering angles when going from positive to negative contrast (see the contrasts for G4-D in Table 1). Very near to the match point (filled triangles in Figure 10), the intensity as a function of q goes through a maximum. This again is to be expected because the forward scattering of monodisperse particles must vanish in the limit of $q = 0$ (see the section Theory and the discussion of Figure 4). The comparison shown in Figure 10 adds therefore further credibility for the fit of $\rho_p(r)$ derived from the partial scattering functions shown in Figure 8 despite the large margin of error for low intensities.

V. Conclusion

The dendrimer G4-D of fourth generation has been analyzed by SANS including contrast variation. The end groups of the dendritic scaffold are deuterated and SANS allows to determine the radial scattering length distribution $\rho_p(r)$ of the segments. The main step in the analysis is the determination of the scattering intensity at different contrast. This allows to determine the partial scattering functions $I_S(q)$, $I_{SI}(q)$, and $I_I(q)$ of the partially deuterated dendrimer (see eq 5). Subsequent inversion of these functions into the real space then leads to the shape function $T(r)$ and the local scattering length density $\rho_p(r)$ (see eq 2). The shape function $T(r)$ is a Gaussian in agreement with the analysis of the protonated dendrimer G4-H. The distribution $\rho_p(r)$ is proportional to the distribution of end groups within the dendrimer. It exhibits a maximum at ca. 2 nm and decays monotonically for larger r. The greatest radial distance for which $T(r)$ is significantly greater than zero is approximately 3 nm. This demonstrates that an appreciable number of end groups must be folded back into the interior of the molecule. This finding is fully compatible with the dense core picture of dendrimers. Moreover, it agrees qualitatively with theoretical predictions.[11] The entire analysis demonstrates in a compelling manner that the dendrimer G4 analyzed in great detail by now[28,29] can fully be understood in terms of the statistical mechanics of polymeric structures.

Acknowledgment. We thank Prof. Dr. Kari Rissanen and Anneli Roulamo (University of Jyväskylä, Finland) for experimental assistance and cooperation in the course of the synthesis of G4-H in the context of a DAAD exchange program. We gratefully acknowledge financial support by the Deutsche Forschungsgemeinschaft (Graduiertenkolleg 366) by the Bundesministerium für Forschung und Technologie (BMBF), by the Roche Diagnostics Co., and by the European Union.

References and Notes

(1) Newkome, G. R.; Moorefield, C. N.; Vögtle, F. *Dendrimers and Dendrons*; Wiley VCH: Weinheim, Germany, 2001.
(2) See, e.g.: Dendrimers III: Design, Dimension, Function. *Top. Curr. Chem.* **2001**, *212*.
(3) Fischer, M.; Vögtle, F. *Angew. Chem., Int. Ed.* **1999**, *38*, 884.
(4) Grayson, S. M.; Frechet, J. M. J. *Chem. Rev.* **2001** *101*, 3819.
(5) Vögtle, F.; Gestermann, S.; Hesse, R.; Schwierz, H.; Windisch, B. *Prog. Polym. Sci.* **2000**, *25*, 987.
(6) de Gennes, P. G.; Hervet, H. *J. Phys. (Paris)* **1983**, *44*, L351.
(7) Lescanec, R. L.; Muthukumar, M. *Macromolecules* **1990**, *29*, 2280.
(8) Mansfield, M. L.; Klushin, L. L. *Macromolecules* **1993**, *26*, 4262.
(9) Mansfield, M. L. *Polymer* **1994**, *35*, 1827.
(10) Murat, M.; Grest, G. S. *Macromolecules* **1996**, *29*, 1278.
(11) Boris, D.; Rubinstein, M. *Macromolecules* **1996**, *29*, 7251.
(12) Cavallo, L.; Fraternali, F. *Chem.—Eur. J.* **1998**, *4*, 927.
(13) Welch, P.; Muthukumar, M. M. *Macromolecules* **1998**, *31*, 5892.
(14) Mansfield, M. L. *Macromolecules* **2000**, *33*, 8043.
(15) Welch, P.; Muthukumar, M. *Macromolecules* **2000**, *33*, 6159.
(16) Karatasos, K.; Adolf, D. B.; Davies, G. R. *J. Chem. Phys.* **2001**, *115*, 5310.
(17) Lyulin, A. V.; Davies, G. R.; Adolf, D. B. *Macromolecules* **2000**, *33*, 6899.
(18) Zacharopoulos, N.; Economou, I. G. *Macromolecules* **2002**, *35*, 1814.
(19) Ballauff, M. Dendrimers III, Design, Dimension, Function. *Top. Curr. Chem.* **2001**, *212*. Ballauff, M. In *Structure and Dynamics of Polymer and Colloidal Systems*; NATO ASI Series 568; Borsali, R., Pecora, R., Eds.; Kluwer Academic Publishers: Dordrecht, The Netherlands, 2002; p 157.
(20) Higgins, J. S.; Benoıt, H. C. *Polymers and Neutron Scattering*; Clarendon Press: Oxford, England, 1994.
(21) Feigin, L. A.; Svergun, D. I. *Structure Analysis by Small-Angle X-ray Scattering and Neutron Scattering*; Plenum Press: New York, 1987.
(22) Pötschke, D.; Ballauff, M.; Lindner, P.; Fischer, M.; Vögtle, F. *Macromolecules* **1999**, *32*, 4079.
(23) Pötschke, D.; Ballauff, M.; Lindner, P.; Fischer, M.; Vögtle, F. *Macromol. Chem. Phys.* **2000**, *201*, 330.
(24) Prosa, T. J.; Bauer, B. J.; Amis, E. J. *Macromolecules* **2001**, *34*, 4897.
(25) Likos, C. N.; Schmidt, M.; Löwen, H.; Ballauff, M.; Pötschke, D.; Lindner, P. *Macromolecules* **2001**, *34*, 2914.
(26) Topp, A.; Bauer, B. J.; Klimash, J. W.; Spindler, R.; Amis, E. J. *Macromolecules* **1999**, *32*, 7226.
(27) Rietveld, I. B.; Bouwman, W. G.; Baars, M. P. L.; Heenan, R. K. *Macromolecules* **2001** *34*, 8380.
(28) Rosenfeldt, S.; Dingenouts, N.; Ballauff, M.; Lindner, P.; Likos, C. N.; Werner, N.; Vögtle, F. *Macromol. Chem. Phys.*, in press.
(29) Likos, C. N.; Rosenfeldt, S.; Dingenouts, N.; Ballauff, M.; Lindner, P.; Werner, N.; Vögtle, F. *J. Chem. Phys.* **2002**, *117*, 1869.
(30) Ohshima, A.; Konishi, T.; Yamanaka, J.; Ise, N. *Phys. Rev. E* **2001**, *64*, 051808.
(31) Ramzi, A.; Scherrenberg, R.; Joosten, J.; Lemstra, P.; Mortensen, K. *Macromolecules* **2002**, *35*, 827.
(32) Imae, T.; Funayama, K.; Aoi, K.; Tsutsumiuchi, K.; Okada, M.; Furusaka, M. *Langmuir* **1999**, *15*, 4076.
(33) Pedersen, J. S. *J. Chem. Phys.* **2001**, *114*, 2839.
(34) Harreis, H.; Likos, C. N.; Ballauff, M. *J. Chem. Phys.*, submitted.
(35) Stephan, H.; Spies, H.; Johannsen, B.; Klein, L.; Vögtle, F. *Chem. Commun.* **1999**, *18*, 1875.

MA020585C